Advances in
Bridge Engineering

ORIGINAL INNOVATION Open Access

The influence of vehicle dynamics on the time-dependent resonances of a bridge

Neda Mostafa[1*], Dario Di Maio[1†], Richard Loendersloot[1†] and Tiedo Tinga[1†]

†Dario Di Maio, Richard Loendersloot, and Tiedo Tinga contributed equally to this work.

*Correspondence: n.mostafa@utwente.nl

[1] Faculty of Engineering Technology, University of Twente, P.O. Box 217, Enschede 7500, The Netherlands

Abstract

In bridge structural health monitoring, the response of the bridge while the vehicle is on the bridge, is called a vehicle-bridge interaction (VBI) response. If the vehicle and the bridge are dynamically coupled, the VBI response depends on the bridge's and the vehicle's dynamic properties. Therefore, the damage detection techniques based on the bridge resonances become questionable due to the dynamic coupling between the bridge and the vehicle. This study investigates the influence of vehicle dynamics on the bridge's time-dependent resonances. Vehicle-Induced Delta Frequency (VIDF) represents the changes in the bridge's time-varying resonances resulting from the vehicle-bridge interaction, while Damage-Induced Delta Frequency (DIDF) accounts for the additional alterations caused by bridge damage. The dynamic interaction between vehicles and bridges (VBIs) is characterized by the frequency ratio between the vehicle (super-system) and the bridge (sub-system). The vehicle frequency is influenced by its dynamics, particularly the suspension systems. Two vehicle models, single suspension and dual suspension vehicles representing passenger trains and freight trains, respectively, are analyzed to assess the significance of vehicle dynamics on VIDF and DIDF. The results demonstrate that both vehicle models experience resonance, which magnifies the dynamic response to damage. However, not all types of vehicles possess the desired dynamic characteristics for effective bridge health monitoring. Trains with single suspension systems exhibit more pronounced changes in the bridge's frequency response. This characteristic makes them more suitable for effective bridge health monitoring and damage detection.

Keywords: Vehicle-bridge interaction, Vehicle dynamics, Damage detection, Instantaneous frequency, Wavelet synchrosqueezed transform

1 Introduction

Degradation of bridge structures due to environmental and traffic factors is inevitable. The collapse of such structures might result in civil and economic casualties. Therefore, a maintenance strategy capable of detecting or even predicting potential failure is crucial to ensure the safety and reliability of bridges. Structural Health Monitoring (SHM) approaches are nowadays prevalent in evaluating structural reliability and damage detection during the service life of civil structures such as bridges. SHM approaches intend to directly or indirectly assess the condition of the bridge structures while they

are in operation. Therefore, the input of the SHM systems is mainly the vehicle-bridge interaction (VBI) response.

A vehicle-bridge interaction (VBI) refers to the dynamic coupling between a bridge and a passing vehicle, resulting in a time-varying process. The dynamic response of the VBI system is influenced by the dynamic properties of both the vehicle and the bridge. Understanding the dynamic interaction between vehicles and bridges is important for both direct and indirect approaches to bridge damage detection. In indirect approaches (Wang et al. 2022; Yang et al. 2004), either the passing vehicle (Zhang et al. 2023) or both the vehicle and the bridge (Sarwar and Cantero 2023) are instrumented. The focus of the current study is on the direct approach, where the VBI response is collected through instrumented bridges.

The VBI models available in the literature have evolved from moving constant force models to complete train-track-bridge interaction models (Zhai et al. 2019). Moving constant force models have been widely used to model the cases where either the weight of the vehicle is much smaller than the weight of the bridge or the vehicle-bridge dynamic coupling is not of interest (Zhai et al. 2019). Therefore, such a model cannot capture the dynamic interaction between the vehicle and the bridge. A more detailed and computationally more expensive multi-body vehicle model is normally implemented to verify safety, ride comfort, and the stability of bridges (Zhu et al. 2017; Zhang et al. 2016; Youcef et al. 2013; Yang and Yau 2017) or to investigate the wheel-rail vertical interactions in case of track irregularities (Zhai and Sun 2008; Zhai and Cai 2016) mainly in the domain of high-speed trains and not focusing on the condition of the bridge. Despite the different interests, the common challenge is the extracting of the dynamic characteristics during the passage of the train, as they are important for condition assessment of the bridge as argued in Mostafa et al. (2021, 2022).

Track irregularities are an important source of complexity in the dynamics response. Short-wavelength track irregularities contribute to noise in trains and the environment (Xin et al. 2019), while long-wave irregularities induce low-frequency vertical oscillations in high-speed trains, where the oscillation frequency is directly proportional to the train's speed (Hung and Hsu 2017), and in cases where the train's speed is low, this frequency can be less than 1 Hz. Since this study is focused on low-speed trains, track irregularities are not further taken into account. It should be noted though that deformation of the bridge due to the presence of the train is not considered to be track irregularity and is taken into account.

There is a rich literature on the implementation of a moving single-stage suspension vehicle on a bridge employing various numerical methods for different purposes such as time-frequency analysis (Hester and Gonzalez 2012), extracting instantaneous frequency (IF) (Roveri and Carcaterra 2012), damage detection (Huseynov et al. 2020), and so on. Li et al. (2003) modeled a moving vehicle with a primary suspension system on a simply supported beam and obtained the fundamental frequency of the bridge utilizing a step-wise solution of the eigenvalue problem at each step of numerical integration. A similar approach was utilized in Law and Zhu (2004) where the bridge resonance is again calculated based on the solution of the eigenvalue problem. Yang et al. (2013) developed a closed-form solution for the frequencies of a VBI system by including only the first mode shape of the system where the vehicle is modeled as a 1-DOF sprung mass.

Cantero et al. (2017) extracted the resonance of a modeled bridge subjected to a moving sprung mass by applying the singular value decomposition technique (SVD) to capture the variation of the bridge resonance (Cantero et al. 2019). Marchesiello et al. (2009) applied continuous wavelet transform (CWT) on the measured acceleration response of a scaled bridge-like structure under a moving train without any suspension, and the time-dependent bridge resonance was successfully extracted. The main objective of the above studies was either applying or developing different approaches to extract the time-dependent resonances of bridges meaning that the influence of the vehicle dynamics on the time-dependent resonances of bridges in healthy or damaged conditions is not fully explored.

The influence of the vehicle dynamics on the dynamic response is addressed in some field measurements. Cantero et al. (2017) experimentally applied CWT to a truck-induced bridge vibration, but no clear pattern of energy distribution in the time-frequency domain was found (Cantero et al. 2017). Xin et al. (2019) proposed an enhanced empirical wavelet transform (EWT) approach, based on the synchro-extracting transform (SET) (Yu et al. 2017), for the time-frequency analysis of a highway bridge under a controlled traffic event; i.e. the passing of two trucks. Li et al. (2020) applied an enhanced short-time Fourier transform (STFT) based on synchro-extracting transform (SET) on the acceleration response of a cable-stayed single-lane highway bridge in Sydney under a passing truck and extracted the instantaneous frequency of the bridge. Regarding railway bridges, He et al. (2011) applied the empirical mode decomposition (EMD) to the forced vibration response of a railway bridge in China, and by means of spectral analysis of the intrinsic mode functions (IMFs). They concluded that the modal frequencies of the bridge change due to the presence of the train. Cantero et al. (2016) applied the Wavelet transform in combination with the modified Littlewood-Paley method on the response of the Skidtrask bridge in Sweden. The proposed method did not successfully identify the time-dependent bridge resonance from the bridge's forced vibration response.

Unlike a few successful time-frequency analyses for highway bridges under a moving truck, railway bridges have not been fully explored yet. It is suggested that the reason for the limited success compared to highway bridge analyses is the vehicle's secondary suspension system which aims to provide passenger ride comfort by isolating the vehicle body from the dynamic loads and vibrations between the wheel and rail (SKF Group 2011). This second-stage suspension system not only affects the train-bridge coupling but also introduces new vibrating modes that can affect the entire VBI system. It is concluded in Cantero et al. (2016) that for railway bridges, the dynamic interaction between the vehicle and the bridge is complex and highly dependent on the mechanical properties of the suspension systems and the distribution of the masses within the vehicle. Many advanced VBI models have been developed, but these have not been applied to analyze the dynamic coupling and the time-dependent resonances of the system for the purpose of condition monitoring or damage identification, which is the objective of the research of the authors. On the one hand, detailed models are sophisticated and computationally expensive to investigate the vehicle-bridge interaction, on the other hand, modeling a multi-axle train as a single or dual suspension point mass may sound oversimplified. However, Fryba (2013) stated that if the vehicle axle base is not comparable with the bridge span length, the vehicle can be modeled as a suspended lumped mass.

Given the earlier-mentioned importance of the number of suspension stages, the current study investigates 1) a single-suspension and, 2) a dual-suspension vehicle model, which are accurate yet simple models to deal with this complicated interaction to investigate the influence of the vehicle dynamics on the healthy and damaged bridge response. Note that freight trains have a single stage of suspension (Iwnicki et al.(2019), locomotives can have one or two suspension stages, whereas passenger trains have two or more suspension stages to provide ride quality (Spiryagin et al. 2016).

Previously, the authors recognized the importance of extracting the instantaneous frequency (IF) and showed in Mostafa et al. (2021) that the Wavelet Synchro-Squeezed Transformation (WSST) outperforms methods like Short-Term Fourier Transformation (STFT) and Continuous Wavelet Transformation (CWT). In Mostafa et al. (2022) it was then shown that the IF can be used to distinguish damage from operational conditions, such as the mass of the train, the temperature, etc. The train dynamics itself were only taken into account to a limited extent: a single sprung mass was used. In the current study, the performance of the damage detection, based on IF extraction via the WSST method and the proposed damage detection method technique will be evaluated for single and dual-suspension vehicle models. This paper therefore investigates the significance of the vehicle dynamics on the dynamic interaction between vehicles and bridges, by extracting the bridge's instantaneous frequency response under intact and damaged conditions. The vehicle-bridge dynamic interaction may mask or magnify the damage influence on the VBI system response. Utilizing those vehicles that magnify the damage leads to a more efficient SHM strategy since the data collection and, subsequently, the data analysis are optimized.

2 Model and data analysis method

The single suspension vehicle model has been used before to investigate the influence of the vehicle dynamics on the bridge resonances (Yang et al. 2013). The influence of the vehicle-bridge coupling on the damaged bridge response has not been explored. For a single suspension vehicle model the determinant frequency ratio is defined as the vehicle (the super-system) frequency over the bridge (the sub-system) frequency. It has been concluded in Yang et al. (2013) that the most substantial interaction occurs at resonance when the car-body bouncing (the vertical oscillation) frequency approaches the bridge frequency. However, the determinant frequency ratio for a dual suspension vehicle model cannot be defined by the car-body to the bridge frequency ratio due to the intermediate bogie suspension. For the dual-suspension vehicle model, the determinant frequency ratio is the bogie (the super-system) over the bridge (sub-system) frequency.

To set up a model with realistic parameters, characteristics of different trains with dual suspension systems are collected from literature sources and presented in Table 1. It can be seen that the car-body bouncing frequency varies in the range 0.52-1.32 Hz. In Eurocode EN 1991-2 (2003), the lower limit of the bridge fundamental frequency is given by $f_r = 23.58L^{-0.592}$ for a span length between 20-100 m, which results in a frequency range of 1.7-4 Hz. Therefore, it can be concluded that these two vibration modes, the car-body bouncing and the bridge bending for dual suspension vehicles, are well-separated and that resonance will not occur. The bogie bouncing frequency range as also presented in Table 1 is 2.3-8.6 Hz which overlaps with the bridge frequency range and can therefore cause resonance. Regarding freight trains, having only a single suspension,

Table 1 Vehicle dynamic properties for dual-suspension trains

Train		Resonance frequency [Hz]		Component mass [kg]	
		Bogie	Car-body	Bogie	Car-body
ETR500-locomotive	(Liu et al. 2009)	4.83	0.65	3896	55976
ETR500-passenger	(Liu et al. 2009)	3.85	0.52	2760	34231
Thalys-237A	(Kouroussis et al. 2011)	5.93	1.03	3261	53442
Thalys-237B	(Kouroussis et al. 2011)	8.6	1.32	1400	28500
Thalys-237A	(Kouroussis et al. 2011)	3.75	1.18	8156	40850
Eurostar-237A	(Kouroussis et al. 2011)	6.5	1.1	3075	54200
Eurostar-237B	(Kouroussis et al. 2011)	4.1	1.01	2363	22000
Eurostar-237B	(Kouroussis et al. 2011)	2.86	0.96	9580	36000
ICE-passenger	(Doménech et al. 2014)	5.84	0.67	2373	34000
ICE-locomotive	(Doménech et al. 2014)	6.6	1.21	5600	61000
Hauling-locomotive	(Spiryagin et al. 2013)	2.36	0.65	14860	87140

the car-body bouncing frequency range is 0.9-4 Hz (Iwnicki et al. 2019), which also overlaps with the bridge frequency range.

Figure 1 presents a single suspension and a dual suspension vehicle model representing a freight train or a locomotive (a) and a passenger train (b) respectively. The variation of the bouncing frequency is also displayed. The current study focuses on the frequency ratio range of 0.55-1.7 for both vehicle models to shed light on the influence of the vehicle dynamics on the coupled system frequency response in two conditions; away-from-resonance, and near-resonance.

All finite element simulations are conducted in two-dimensional space in ABAQUS where Euler-Bernoulli beam elements are used. An extended version of a simply supported beam is used to simulate the bridge numerically. The bridge model is extended to obtain the bridge's free vibration, while the mass is not present on the bridge. To this end, an approaching and leaving length are added before and after the bridge to properly locate the mass during the forced and free vibration phases. The extension sections are pinned to the ground, and they allow to generate the bridge response while the vehicle is approaching and leaving the bridge. The bridge model (i.e. the center part of 80 m) has 1600 rectangular beam elements of $A = 0.4$ m^2 cross section area and with Young's

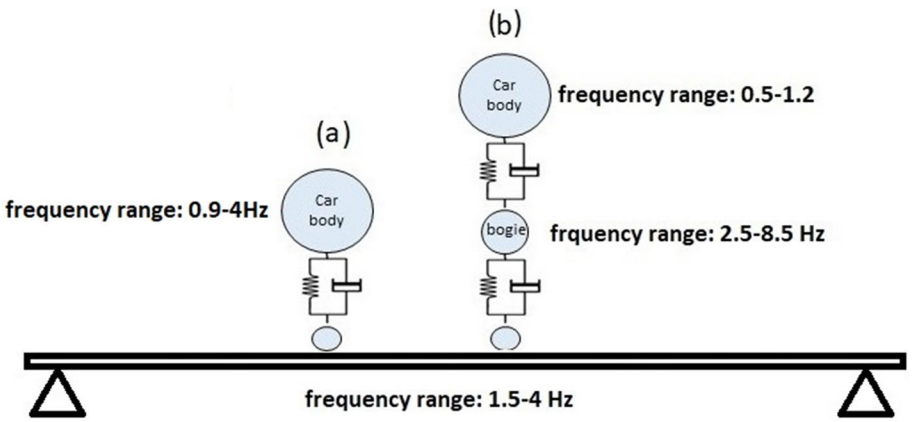

Fig. 1 The vehicle models used in the current study

modulus $E = 210$ GPa, density $\rho = 7860$ kg/m^3. The fundamental frequency of the bridge model is 2.99 Hz. Rayleigh damping with the coefficients $\alpha = 0.001$ and $\beta = 0.001$ is added to increase the stability of the solver and viscous damping with a damping coefficient of $C = 10,000$ N·s/m (well below the critical damping: $\zeta \approx 4 \cdot 10^{-3}$) is added to limit the motion of the car body.

The damage detection concept proposed by the authors in Mostafa et al. (2022) implies that the bridge's forced vibration response is more sensitive to damage than the free vibration response. The proposed damage-sensitive feature is the bridge instantaneous frequency and the magnitude variation has been introduced. The magnitude variation δ quantifies the deviation of the measured instantaneous frequency for a VBI system, $\mathcal{F}_m$, from the baseline instantaneous frequency of the VBI system, $\mathcal{F}_b$.

$$\delta(\mathcal{F}_b, \mathcal{F}_m) = \frac{\sum_{i=1}^{n-1} \left(\frac{1}{2}\left(\mathcal{F}_{b,i} + \mathcal{F}_{b,i+1}\right)\Delta t - \frac{1}{2}\left(\mathcal{F}_{m,i} + \mathcal{F}_{m,i+1}\right)\Delta t \right)}{\sum_{i=1}^{n-1} \left(\frac{1}{2}\left(\mathcal{F}_{b,i} + \mathcal{F}_{b,i+1}\right)\Delta t - f_b \Delta t \right)} = \frac{\text{DIDF}}{\text{VIDF}} \tag{1}$$

where f_b refers to the bridge fundamental frequency, which is constant in time and thus a scalar value. In the transient phase, the bridge frequency continuously changes in time (as defined by the time steps $i = 1 : n$) depending on the location of the vehicle. The denominator of Eq. (1) calculates the area in the frequency versus time plot bounded by $\mathcal{F}_b$ and f_b for the intact bridge. It, therefore, corresponds to the change of the baseline instantaneous frequency of the intact bridge induced by the operational condition and is referred to as the Vehicle Induced Delta Frequency (VIDF). Once the instantaneous frequency of a measured response differs from the baseline, which would be the case when damage is present, then the bounded area between $\mathcal{F}_b$ and $\mathcal{F}_m$ is a nonzero value that quantifies the magnitude variation. The numerator of Eq. (1) is therefore referred to as the Damage Induced Delta Frequency (DIDF). The magnitude variation δ thus is the ratio between the bridge instantaneous frequency variation induced by damage and the bridge instantaneous frequency variation induced by the vehicle.

3 Single suspension vehicle model

3.1 The influence of the vehicle dynamics on the intact bridge instantaneous frequency

The single suspension vehicle model represents a locomotive or freight train that in practice has a larger mass than the passenger trains. For the single suspension vehicle model the natural frequency of the vehicle (the super-system) is $\sqrt{(k_{car}/m_{car})}$ where the mass of the car is about 15–35% of the bridge mass. In the current study, the vehicle mass ranges from 40 tons to 80 tons, denoted as m1 to m9. The mass values are distributed within this range with a step size of 5 tons. The car mass is set such that it covers the common range of car masses presented in Table 1. Having the vehicle mass and the target frequency ratio range, the vehicle stiffness can be calculated. In the current study, the vehicle stiffness variation range is 9 MN/m to 40 MN/m, denoted as k1 to k9. These stiffness values are distributed within the specified range, with a step size of 3.875 MN/m. Therefore, by taking into account the 9 mass variations (m1 to m9) and the 9 stiffness variations (k1 to k9), this study involves the modeling of a total of 81 VBI systems.

Once the vehicle model properties are set, the influence of the vehicle dynamics on the instantaneous frequency of the intact bridge model is investigated. There are two approaches to obtain the instantaneous frequencies of VBI systems: 1) step-wise modal analysis and, 2) dynamic implicit analysis. The step-wise modal analysis aims to calculate the system resonances of the VBI system depending on the location of the vehicle on the bridge. The step-wise approach is computationally affordable, but it is a static approach that is not able to capture the local variation of the instantaneous frequency due to the presence of damage. A dynamic analysis is computationally expensive, yet it provides a high-resolution instantaneous frequency. Therefore, the step-wise modal analysis is used to quantify the intact bridge resonances, whereas the dynamic implicit integration scheme is used to calculate the damaged bridge acceleration response and investigate the influence of the vehicle dynamics on the instantaneous frequency of the damaged bridge.

The step-wise modal analysis starts by locating the vehicle on the left support of the bridge. For the next step, the vehicle is located at 10 m distant from its previous location. The steps are repeated until the vehicle reaches the bridge's right support. At each step, the eigenfrequencies of the system corresponding to the car-body bouncing and the bridge resonance are collected as a numerical array. Figure 2 presents a set of results of the step-wise modal analysis for the single suspension vehicle model with constant stiffness (k4) and variable mass (m1 to m9). The horizontal axis is labeled as the relative vehicle location which represents the ratio of the distance traveled by the vehicle on the bridge and the bridge length. The light blue area corresponds to the VIDF, as defined in Eq. (1), since the VIDF is the area enclosed by the instantaneous frequency and the bridge frequency (dashed line in Fig. 2).

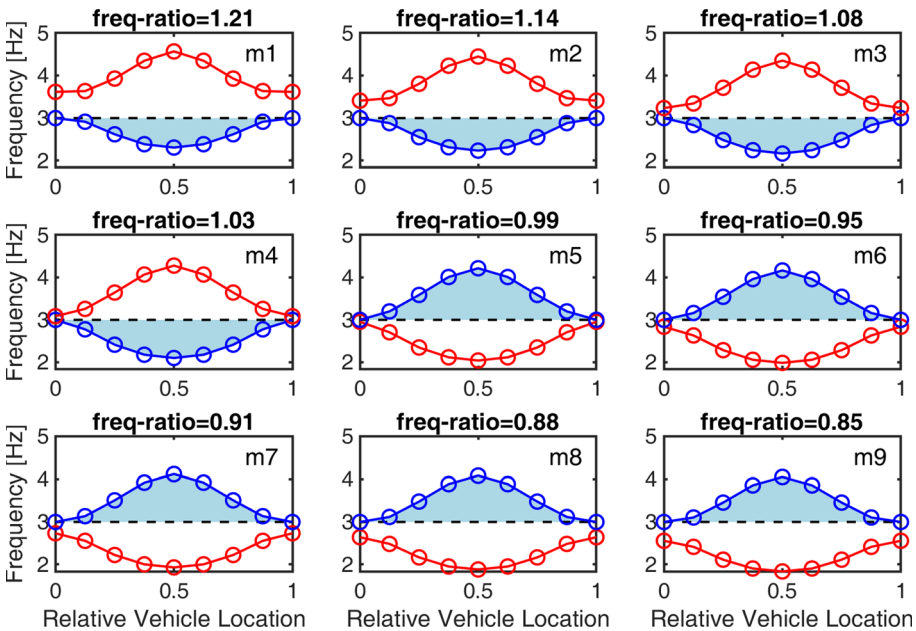

Fig. 2 The bridge (blue marker) and the vehicle (red marker) frequency variation during a vehicle passage for a constant vehicle stiffness (k4, $k = 20.625$ MN/m) and nine different vehicle mass values (indicated by the resulting car-bridge frequency ratio). The bridge's fundamental frequency is displayed as a dashed black line. The light blue area corresponds to the VIDF

The top-left corner subplot of Fig. 2 represents a VBI system with the first two resonance frequencies of 2.9 Hz and 3.6 Hz corresponding to the bridge bending resonance frequencies and the car bouncing respectively. These values are visible when the vehicle is located at the left support. The bridge bending frequency (blue curve) appears as the first mode of the coupled system. While the vehicle moves towards the mid-span the bridge frequency decreases to 2.3 Hz when the vehicle is at the mid-span and again comes back to the initial value (2.9Ḣz) when the vehicle arrives at the right support. The vehicle frequency (red curve) increases to 4.5 Hz when the vehicle is located at the mid-span, and when the vehicle comes back to the right support the frequency also comes back to the initial value (3.6 Hz). This pattern is valid as long as the frequency ratio is larger than 1. Once the frequency ratio comes close to unity, this pattern is changed. It can be seen in the middle row, center plot of Fig. 2 that the vehicle frequency is now the first (lowest) mode of the coupled system and it decreases when the vehicle moves towards the bridge mid-span.

The way the resonance frequencies change can be explained by the relative motion of the bridge and the vehicle. The first resonance mode of the bridge-vehicle system is comparable to an in-phase motion of the vehicle mass and the bridge: the car body moves in the same direction as the bridge and follows its vertical displacement, as shown in Fig. 3a. As a result, the instantaneous resonance frequency of the bridge decreases when the mass moves toward the mid-span position, similar to the effect of an added mass. The second resonance is comparable to an out-of-phase motion, where the vehicle mass and bridge move in opposite directions, as shown in Fig. 3b. This is similar to the effect of an added stiffness and hence results in an increase of the instantaneous resonance frequency when the mass moves toward the mid-span position.

The VIDF has been proposed to quantify the influence of vehicle dynamics on the vehicle-bridge coupled system. The VIDF as introduced in Eq. (1) calculates the area bounded by $\mathcal{F}_b$: the bridge instantaneous frequency (blue curves in Fig. 2) and f_b the bridge fundamental frequency (the dashed black line at 2.99 Hz in Fig. 2) for the intact bridge. It can be observed in Fig. 2 that the VIDF increases when the frequency ratio approaches unity and decreases when the frequency ratio gets smaller or larger than unity.

The VIDF is calculated for all 81 VBI systems and plotted against the frequency ratio in Fig. 4. Each marker in Fig. 4 corresponds to one of the VBI systems, where the color

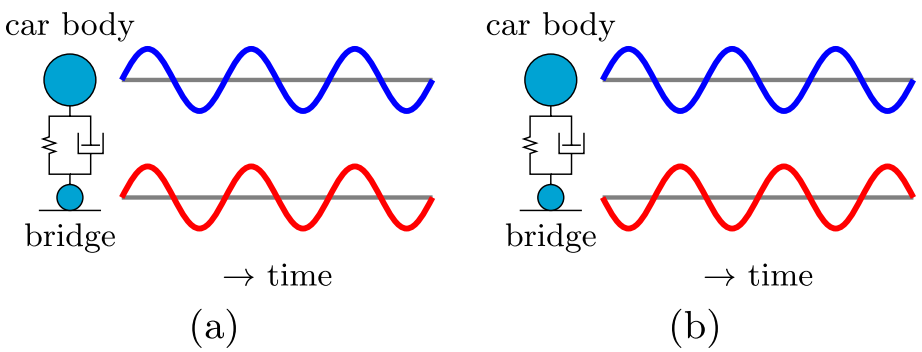

Fig. 3 Mode shapes retrieved from the step-wise eigenfrequency analyses show that the car and the bridge move **a** in-phase or **b** out-of-phase

indicates the stiffness and the size of the marker the mass ratio (small: m1; large: m9). The solid markers correspond with the case shown in Fig. 2 (k4, m1-m9). As previously observed from Fig. 2, the maximum value for the VIDF is reached at the resonance condition, where the frequency ratio equals unity.

Figure 4 shows in addition that the VIDF drops quicker when moving away from resonance for the VBI systems with a frequency ratio larger than unity compared to VBI systems with a frequency ratio smaller than unity. This is illustrated by the non-equal spacing between markers below and above resonance for the purple, solid markers (case k4, m1-m9). The VIDF for a given absolute distance from the resonance condition is lower for a frequency ratio higher than unity compared to that of a frequency ratio lower than unity. This behavior can be attributed to the different effects of added mass versus added stiffness on the change of the instantaneous frequency $\mathcal{F}_b$.

3.2 The influence of the vehicle dynamics on the damaged bridge instantaneous frequency

The numerator of Eq. (1) introduces the Damage Induced Delta Frequency, DIDF. The main objective of this section is to quantify DIDF for the modeled VBI systems and investigate the influence of the vehicle dynamics on the DIDF. The question is in which situation the DIDF is magnified and thus when optimal conditions for bridge damage detection occur.

The numerical model of the bridge in the current study consists of 1600 elements of 50 mm long. To implement damage, the stiffness of 16 elements along the bridge midspan is reduced by 50%. The total length of the damaged area is thus about 1% of the bridge span length. The damage severity and length are kept constant for all step-wise modal analyses. The same mass and stiffness variations (9×9=81 VBI systems) are used as in the previous section. A more detailed study on the effect of various damage scenarios is presented in Mostafa et al. (2022).

Among the 81 vehicle-bridge interaction (VBI) systems studied, two examples were selected to illustrate the instantaneous frequencies of the bridge in both intact and damaged conditions. Figure 5a shows the instantaneous frequency of the VBI system

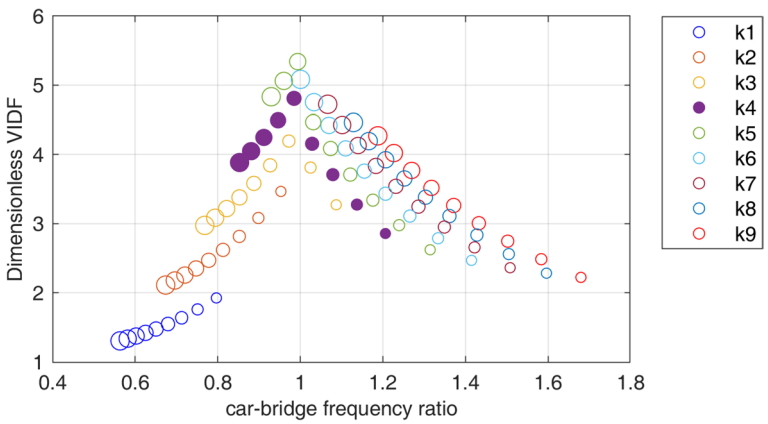

Fig. 4 VIDF versus car-bridge frequency ratio. Each color corresponds to the stiffness k1 to k9, while the size of the marker represents m1 (small) to m9 (large). The set of solid markers is used as an example for the step-wise analysis

with the lowest car-bridge mass ratio of 0.16 (m1) and the highest car-bridge frequency ratio of 1.68 (corresponding with the highest stiffness case k9). This VBI system exhibits an in-phase regime, where the vehicle behaves as an added mass on the bridge, as depicted Fig. 3a. In Fig. 5a, the instantaneous frequency of the intact bridge is represented by the black curve, while the red curve represents the instantaneous frequency of the damaged bridge. The DIDF represents the bounded area between the frequency curves of the intact and damaged bridges. In Fig. 5a, it is evident that the damaged bridge frequency curve (red curve) exhibits a local reduction around the area of damage. This reduction in the bridge's instantaneous frequency is attributed to the decreased stiffness of the damaged elements and the additional mass introduced by the vehicle.

A VBI system with the lowest vehicle-bridge frequency ratio is chosen as a second example. The instantaneous frequency of the VBI system with a car-bridge mass ratio of 0.32 (m9) and a car-bridge frequency ratio of 0.55 (the lowest frequency ratio, and lowest stiffness case k1) is shown in Fig. 5b. This VBI system represents an out-of-phase regime, where the vehicle mass counteracts the bridge motion. Again, the black curve represents the intact bridge's instantaneous frequency, while the red curve represents the damaged bridge's instantaneous frequency. Unlike Fig. 5a, where a larger frequency reduction was observed, Fig. 5b shows only a marginal frequency reduction around the damage location. This is because the vehicle is effectively acting as an added stiffness in this case.

Only a subset of the 81 VBI systems is used to investigate the influence of the vehicle dynamics on the Damage Induced Delta Frequency (DIDF), considering the computational time of each individual dynamic simulation. The dynamic simulations are performed for 5 VBI systems with the highest vehicle stiffness value (k9, k =3.6MN/m) and for 5 VBI systems with the lowest vehicle stiffness value (k1, k = 0.9Mn/m). Figure 6 displays the resulting DIDF for these two times 5 VBI systems, where the blue markers correspond with the lowest stiffness (k1) and the red markers with the highest stiffness (k9).

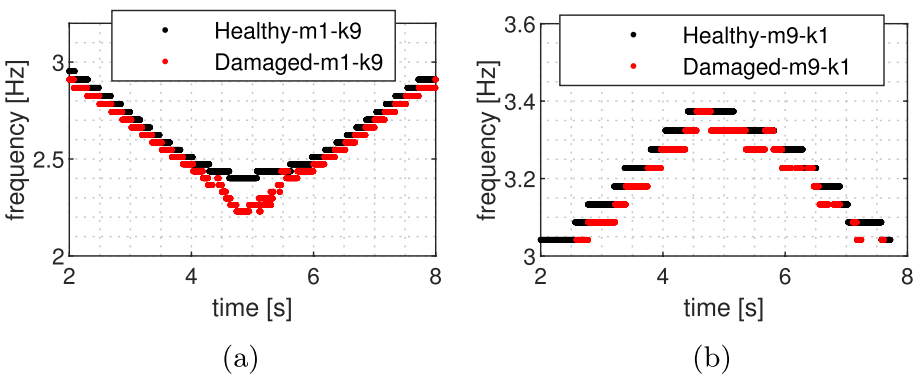

Fig. 5 The intact and the damaged bridge instantaneous frequency ridges are displayed in black and red respectively, for two VBI systems; **a** the VBI system with a car-bridge mass ratio of 0.16 (m1) and a car-bridge frequency ratio of 1.68 and, **b** the VBI system with a car-bridge mass ratio of 0.32 (m9) and a car-bridge frequency ratio of 0.55

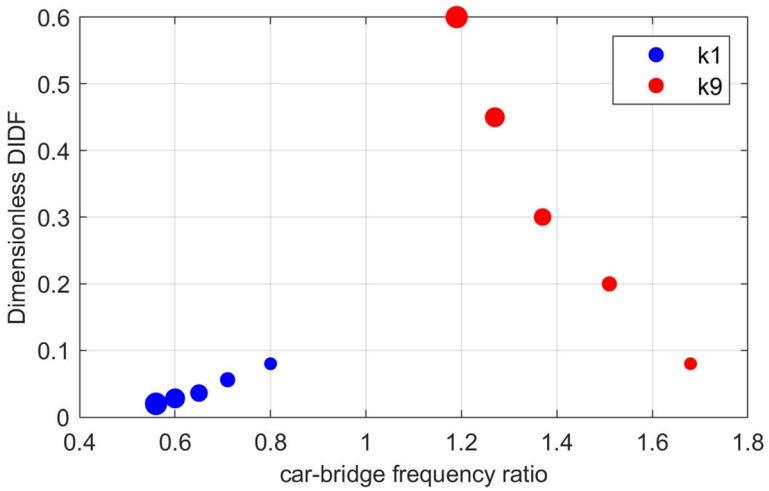

Fig. 6 DIDF versus car-bridge frequency ratio. Blue markers correspond with k1, red with k9, while the size of the markers represents the mass ratio: m1 (smallest marker size), m3, m5, m7, and m9 (largest marker size)

The observed pattern of the DIDF is similar to that of the VIDF. A maximum is reached if the frequency ratio is unity. Moving away from resonance yields a decrease of the DIDF. The VBI systems having a frequency ratio lower than unity correspond to an out-of-phase motion of the bridge and vehicle, while the VBI systems with a frequency ratio higher than unity correspond to an in-phase motion of the bridge and vehicle. The size of the marker indicates the car-bridge mass ratio (m1, m3, m5, m7, and m9), which for both stiffnesses k1 and k9 is increasing with increasing frequency ratio. Similar to the VIDF, the DIDF drops quicker when moving away from the resonance condition for the in-phase case (frequency ratio > 1), compared to the out-of-phase case (frequency ratio < 1). The resonance condition is not reached for both sets of VBI systems. The mass ratio for the specific combination of bridge and train types under investigation would become very unrealistic. However, it can still be observed from the graph that the lower stiffness case (k1) shows significantly lower values for the DIDF than the higher stiffness case (k9).

It can be concluded that for a unique damaged bridge, different vehicles trigger the damage differently. Furthermore, the DIDF for VBI systems having a frequency ratio larger than unity seems to be larger than for the VBI systems having a frequency ratio less than unity. Finally, being close to resonance (i.e. frequency ratio equal to unity) magnifies the response to damage.

4 Dual suspension vehicle model

4.1 The influence of the vehicle dynamics on the intact bridge instantaneous frequency ridge

This section investigates the VIDF due to the primary suspension stage of the dual suspension vehicle model displayed in Fig. 1. In this figure, also the common frequency range of the car body and the bogie system found in the literature are presented. As mentioned previously, the car-body bouncing frequency for dual suspension vehicles and the bridge bending frequency are well-separated, thus, resonance will not occur.

However, the bogie bouncing frequency overlaps with the bridge frequency range and here resonance can occur.

For the dual suspension vehicle model, the car dynamics contribute to the vehicle-bridge dynamic interaction through the bogie. Through the current study, the frequency ratio is the benchmark to compare the VBI systems with different vehicle models i.e. different super-systems. For the single suspension vehicle model the car and for the dual suspension vehicle model the combination of the bogie and the car dynamics serve as the super-system. Therefore, for the dual suspension vehicle model, the influence of the primary suspension is investigated by keeping the car mass and stiffness constant and changing the bogie properties. Also, the influence of the secondary suspension is explored by keeping the bogie properties constant and changing the car properties.

The influence of the primary suspension is presented here where the car mass (40 tons) and the car stiffness (0.91 Mn/m) are constant and the bogie mass and the bogie stiffness are tuned such that the frequency ratio ranges from 0.6-1.5. The bogie stiffness variation range is 1.268-3.96 MN/m and the bogie mass variation range is 6,117-13,677 kg. Each range is again divided into 9 steps, yielding a total of $9 \times 9 = 81$ VBI systems. Note that the car bouncing frequency is smaller than 1 Hz and it always appears as the first mode, which corresponds with the actual situation in passenger trains to ensure passenger comfort during the ride.

A step-wise analysis, similar to the one presented in Section 3 is done first. The results are shown in Fig. 7, which displays the bridge and the bogie resonances in blue and red respectively for a fixed bogie mass and all bogie stiffnesses k1 to k9, covering the frequency ratio from 0.78 (top left subplot) to 1.18 (bottom right subplot).

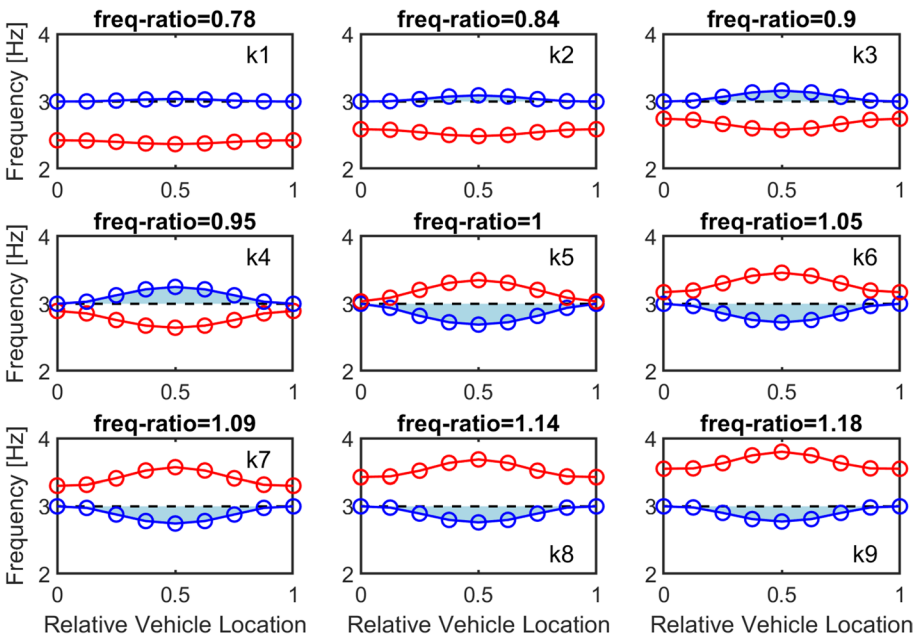

Fig. 7 The bridge (blue marker) and the vehicle (red marker) frequency variation during a dual suspension vehicle passage for a constant bogie mass and nine different bogie stiffness values k1-k9. The bridge's fundamental frequency is displayed as a dashed black line. The light blue area corresponds to the VIDF

The top left corner plot of Fig. 2 and the bottom right corner plot of Fig. 7, show two VBI systems having similar frequency ratios (around 1.18). It can be seen that the single suspension vehicle in comparison with the dual suspension vehicle model shows more dynamic interaction which yields a higher VIDF, which is visualized in both graphs by the light blue area enclosed by the blue curve and the black dashed line.

The VIDF as a function of the frequency ratio for all 81 VBI systems is presented in Fig. 8. The different colors refer to the different bogie stiffness cases k1 to k9, while the size of the markers refers to the bogie-bridge mass ratio cases m1 (small) to m9 (large). The pattern for the dual suspension vehicle model is similar to the pattern observed for the single suspension vehicle model (see Fig. 4). The maximum VIDF occurs when approaching a frequency ratio of one near resonance conditions, while the VIDF drops when moving away from a frequency ratio of unity. In out-of-phase motion regimes when the system is away from resonance, the VIDF tends to zero, whereas for in-phase regimes the VIDF tends to 0.4 far from resonance. This means that even for passenger trains with a double-stage suspension when the frequency ratio is larger than unity, the vehicle dynamics affect the bridge's instantaneous frequency. At resonance, VIDF reaches the maximum values which are lower than the maxima observed in Fig. 4 of the VIDF at resonance of the single suspension vehicle model. Although the mass of the entire system is (nearly) the same for the single suspension and dual suspension systems, the car body has a more limited contribution to the change of the instantaneous frequencies, and hence the VIDF, compared to the bogie. Effectively, the motion of the car body is largely isolated from the bridge and bogie motion due to the low stiffness of the secondary suspension.

Another set of 81 (9×9) VBI systems is analyzed to further support the finding that the dual suspension system has a lower influence on the VIDF compared to the single suspension system. The objective is now to investigate the impact of car mass and car stiffness on the bridge frequency rather than the bogie mass and bogie stiffness. The bogie mass (9580 kg) and the bogie stiffness (1.268 MN/m) are considered constant. The variation in car dynamics is examined for the bogie-bridge frequency ratio ranging from 0.8 to 1.4 by varying the car stiffness ranges in 9 steps from 0.9 to 3.6 MN/m, while the car

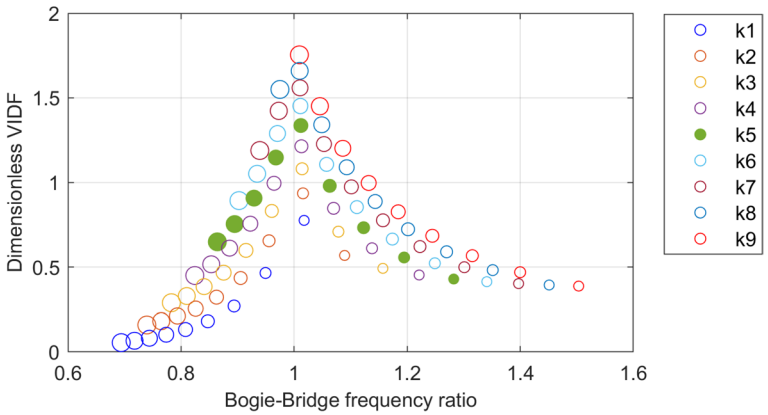

Fig. 8 VIDF versus bogie-bridge frequency ratio. Each color corresponds to the primary stiffness (k1 to k9), while the size of the marker represents bogie mass (m1: small; m9: large). The solid markers show the case k5, m1-m9

mass varies in 9 steps between 40 and 80 tons. The VIDF values versus the frequency ratio, resulting from these analyses, are presented in Fig. 9.

The blue markers in Fig. 9, corresponding with the lowest secondary suspension stiffness and covering the full range of car body mass variation, all nearly coincided and result in the same VIDF value. This indicates that the car body mass has a very limited influence on the VIDF. The red markers, corresponding with the highest secondary suspension stiffness, show a larger variation in VIDF, but this is still a low amount of variation compared to the variation observed in Fig. 8. In addition, the maximum value for the VIDF near resonance is also lower than in case the bogie mass and stiffness vary. Additionally, Fig. 9 reveals that the variation in car body mass has a marginal effect on the VIDF for systems operating away from resonance conditions.

4.2 The influence of the vehicle dynamics on the damaged bridge instantaneous frequency

Based on the previous analysis, it can be concluded that the bogie dynamics play a crucial role in the vehicle-bridge dynamic interaction for passenger trains. Furthermore, it was observed that vehicles operating in the in-phase regime (frequency ratio > 1) amplify the VIDF more than in the out-of-phase regime (frequency ratio < 1). In this section, only the influence of the bogie dynamics on the DIDF for the dual suspension vehicle models in the in-phase regime is investigated. The vehicle model is configured with a constant bogie stiffness of 3.96 MN/m (k9) and a variation of the bogie mass between 6,117-13,677 kg. Only 5 steps (m1, m3, m5, m7, and m9) are used to limit the computational time. Figure 10 shows the corresponding DIDF. A similar pattern as in Fig. 6 can be observed in Fig. 10. The DIDF value drops when moving away from the resonance condition and seems to converge to approximately 0.1. The difference between the single-suspension and dual-suspension systems reduces with increasing frequency ratio, but close to resonance, the damage-induced variation in the instantaneous frequency is significantly larger for the single-suspension system. This observation is in line with the earlier observation that the change of the VIDF is also lower for the dual-suspension systems compared to that of the single-suspension systems.

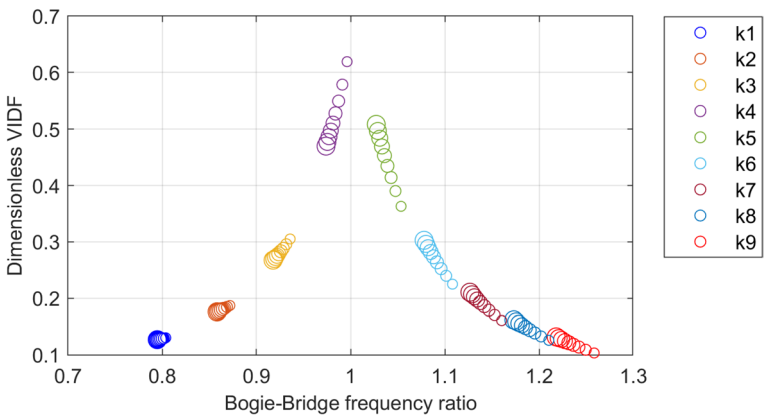

Fig. 9 VIDF versus bogie-bridge frequency ratio. Each color corresponds to the secondary stiffness (k1 to k9), while the size of the marker represents car mass (m1: small; m9: large)

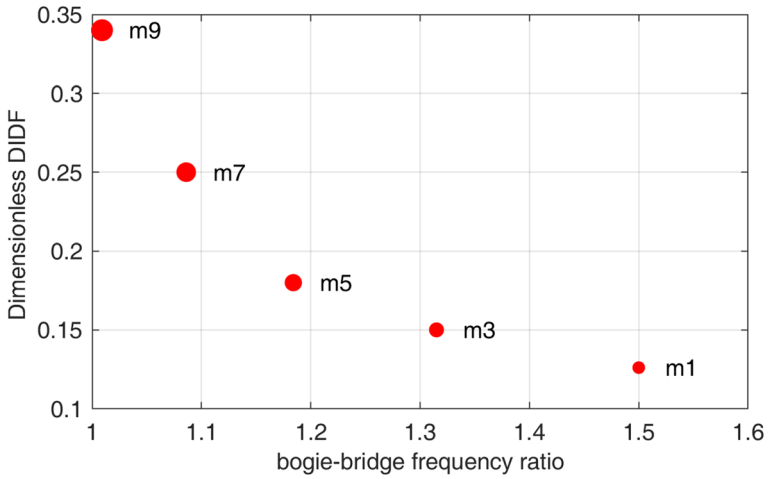

Fig. 10 DIDF versus bogie-bridge frequency ratio. Results of the highest stiffness case (k9) are shown for mass ratios m1 (smallest marker size), m3, m5, m7, and m9 (largest marker size)

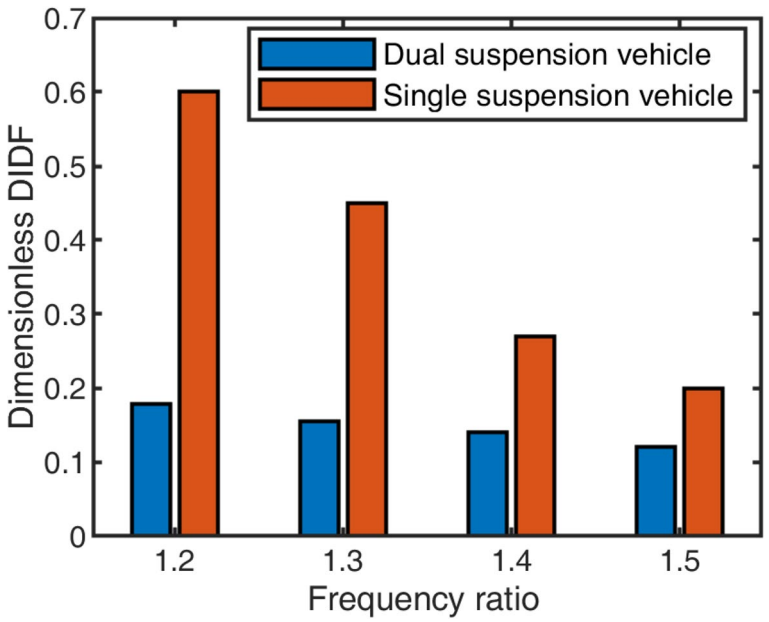

Fig. 11 The DIDF of the single suspension and the dual suspension vehicle models for frequency ratios of 1.2 and 1.5

5 Discussion

The dynamic properties of the single-suspension vehicle model cannot be directly compared to those of the dual-suspension vehicle model. However, the frequency ratio between the super system (the vehicle) and the sub-system (the bridge) serves as a criterion for representing and comparing the vehicle-bridge dynamic interaction. Figure 11 provides a concise summary of the findings presented in Figs. 6 and 10 illustrating the DIDF for both the single suspension and dual suspension vehicle models. The figure specifically focuses on the in-phase regime for which the frequency ratio ranges from 1.2

to 1.5. In Fig. 11 it is evident that as the vehicle approaches the resonance condition the DIDF increases for both vehicle models. The figure also clearly demonstrates a significant difference in DIDF between the single-suspension vehicle model representing freight trains or single locomotives and the dual-suspension vehicle model representing passenger trains. At a frequency ratio of 1.2, Fig. 11 displays that the DIDF of the dual suspension vehicle is approximately 0.18 while, this value for the single suspension vehicle is approximately 0.6 which is roughly three times larger. Note that in both cases the total mass of the vehicle is the same.

This discrepancy in DIDF values can be attributed to the distinct characteristics of the suspension systems employed in each vehicle model. Compared to dual-suspension vehicles, the single-suspension vehicle exhibits a higher impact on the bridge dynamics which translates into a larger change of the bridge's instantaneous frequency when damage is present. This enhanced sensitivity enables the detection of smaller deviations in the bridge's frequency response, thereby facilitating the identification of potential damage in an earlier stage. These findings serve as guidelines for the design of bridge health monitoring systems, combined with a dedicated approach, which for example involves the deployment of dedicated vehicles designed specifically for the purpose of structural assessment.

6 Conclusion

The dynamic interaction between a vehicle and a bridge is numerically investigated for two vehicle models: a single-suspension and a dual-suspension vehicle. The instantaneous frequencies of the vehicle-bridge interaction (VBI) models for an intact and damaged bridge are extracted by performing a series of step-wise modal analyses and a series of transient response analyses. The Vehicle-Induced Delta Frequency (VIDF) was proposed earlier to quantify the influence of the vehicle dynamics on the response of the intact bridge. The Damage-Induced Delta Frequency (DIDF) was proposed as a damage-sensitive feature to quantify the influence of vehicle dynamics on damage detection. The investigation of the Vehicle-Bridge Interaction (VBI) system response, conducted near resonance conditions, focused on a single-span simply supported bridge in the context of low-speed train operations. From this analysis, the following conclusions can be drawn:

- To ensure accurate and reliable bridge health monitoring and damage detection, it is crucial to select suitable train types. Not all types of trains possess the desired dynamic characteristics for effective bridge health monitoring.
- Trains with single suspension systems cause more pronounced changes in the bridge's frequency response than dual suspension trains, specifically the Vehicle-Induced Delta Frequency (VIDF) and Damage-Induced Delta Frequency (DIDF). This phenomenon can be attributed to the concept of interacting mass. In single suspension systems, the entire mass of the train, including the car body, interacts directly with the bridge. In contrast, dual suspension systems decouple the car body from the bridge, leading to a reduction in the mass interaction between the train and the bridge.

- In the case of dual-suspension vehicles, the outcomes demonstrate that the influence of the vehicle mass on the bridge frequency is negligible compared to the mass of the bogie. This observation aligns with the intended role of the secondary suspension system, which is primarily focused on enhancing ride comfort by effectively decoupling the car body from the undesired vibrations of the subsystems. Hence, when the objective is to analyze the impact of vehicle dynamics on the bridge's instantaneous frequency (VIDF) for dual-suspension vehicles, it is essential to focus on the characteristics and properties of the bogie rather than the car mass.
- Both vehicle models experience resonance, which magnifies the dynamic response to damage. This phenomenon highlights the importance of considering resonance effects in bridge health monitoring strategies for both single-suspension and dual-suspension vehicles.

Authors' contributions
N.M. mainly contributed to the research and numerical studies, and R.L. contributed to the discussion on the results, formulation of ideas, and the writing, while T.T., and D.D. mainly contributed as support during the writing process.

Funding
This study has been performed as part of the DESTination RAIL project Decision Support Tool for Rail Infrastructure Managers. The DESTination RAIL project has received funding from the European Union's Horizon 2020 research and innovation program under grant agreement No 636285.

Availability of data and materials
The University of Twente is the owner of the research data. The research data can be available considering the data management policy of the University of Twente.

Code availability
The University of Twente is the owner of the code. The code can be available considering the data management policy of the University of Twente.

Declarations

Ethics approval and consent to participate
Not applicable.

Consent for publication
Not applicable.

Competing interests
The authors have no competing interests.

Received: 29 June 2023 Accepted: 7 September 2023
Published online: 09 October 2023

References

Cantero D, Ülker Kaustell M, Karoumi R (2016) Time-frequency analysis of railway bridge response in forced vibration. Mech Syst Signal Process 76–77:518–530. https://doi.org/10.1016/j.ymssp.2016.01.016
Cantero D, Hester D, Brownjohn J (2017) Evolution of bridge frequencies and modes of vibration during truck passage. Eng Struct 152:452–464. https://doi.org/10.1016/j.engstruct.2017.09.039
Cantero D, McGetrick P, Kim CW et al (2019) Experimental monitoring of bridge frequency evolution during the passage of vehicles with different suspension properties. Eng Struct 187:209–219. https://doi.org/10.1016/j.engstruct.2019.02.065
Doménech A, Museros P, Martínez-Rodrigo MD (2014) Influence of the vehicle model on the prediction of the maximum bending response of simply-supported bridges under high-speed railway traffic. Eng Struct 72:123–139. https://doi.org/10.1016/j.engstruct.2014.04.037
Fryba L (2013) Vibration of solids and structures under moving loads. Noordhoff International Publishing, Groningen
He XH, Hua XG, Chen ZQ et al (2011) EMD-based random decrement technique for modal parameter identification of an existing railway bridge. Eng Struct 33(4):1348–1356. https://doi.org/10.1016/j.engstruct.2011.01.012

Hester D, Gonzalez A (2012) A wavelet-based damage detection algorithm based on bridge acceleration response to a vehicle. Mech Syst Signal Process 28:145–166. https://doi.org/10.1016/j.ymssp.2011.06.007
Hung CF, Hsu WL (2017) Influence of long-wavelength track irregularities on the motion of a high-speed train. Veh Syst Dyn 56(1):95–112. https://doi.org/10.1080/00423114.2017.1346261
Huseynov F, Kim C, Obrien EJ et al (2020) Bridge damage detection using rotation measurements - experimental validation. Mech Syst Signal Process 135. https://doi.org/10.1016/j.ymssp.2019.106380
Iwnicki S, Spiryagin M, Cole C et al (2019) Handbook of Railway Vehicle Dynamics. Handbook of Railway Vehicle Dynamics. CRC Press. https://doi.org/10.1201/9780429469398
Kouroussis G, Verlinden O, Conti C (2011) Free field vibrations caused by high-speed lines: Measurement and time domain simulation. Soil Dyn Earthquake Eng 31(4):692–707. https://doi.org/10.1016/j.soildyn.2010.11.012
Law SS, Zhu XQ (2004) Dynamic behavior of damaged concrete bridge structures under moving vehicular loads. Eng Struct 26(9):1279–1293. https://doi.org/10.1016/j.engstruct.2004.04.007
Li J, Zhu X, Ss Law et al (2020) Time-varying characteristics of bridges under the passage of vehicles using synchroextracting transform. Mech Syst Signal Process 140. https://doi.org/10.1016/j.ymssp.2020.106727
Li JZ, Su MB, Fan LC (2003) Natural frequency of railway girder bridges under vehicle loads. J Bridge Eng 8(4):199–203. https://doi.org/10.1061/(Asce)1084-0702(2003)8:4(199)
Liu K, Roeck GD, Lombaert G (2009) The effect of dynamic train-bridge interaction on the bridge response during a train passage. J Sound Vib 325(1–2):240–251
Marchesiello S, Bedaoui S, Garibaldi L et al (2009) Time-dependent identification of a bridge-like structure with crossing loads. Mech Syst Signal Process 23(6):2019–2028. https://doi.org/10.1016/j.ymssp.2009.01.010
Mostafa N, Di Maio D, Loendersloot R et al (2021) Extracting the time-dependent resonances of a vehicle-bridge interacting system by wavelet synchrosqueezed transform. Struct Control Health Monit. https://doi.org/10.1002/stc.2833
Mostafa N, Maio DD, Loendersloot R et al (2022) Railway bridge damage detection based on extraction of instantaneous frequency by wavelet synchrosqueezed transform. Adv Bridge Eng 3(1):12. https://doi.org/10.1186/s43251-022-00063-0
Roveri N, Carcaterra A (2012) Damage detection in structures under traveling loads by Hilbert-Huang transform. Mech Syst Signal Process 28:128–144. https://doi.org/10.1016/j.ymssp.2011.06.018
Sarwar MZ, Cantero D (2023) Vehicle assisted bridge damage assessment using probabilistic deep learning. Measurement 206. https://doi.org/10.1016/j.measurement.2022.112216
SKF. Railway technical handbook: a handbook for the industrial designer and operator. Vol. 1. Axleboxes, wheelset bearings, sensors, condition monitoring, subsystems and services, Volume 1. SKF; 2011. https://books.google.nl/books?id=8xkUtwAACAAJ. ISBN: 9789197896634.
Spiryagin M, Sun YQ, Cole C et al (2013) Development of a real-time bogie test rig model based on railway specialised multibody software. Veh Syst Dyn 51(2):236–250. https://doi.org/10.1080/00423114.2012.724176
Spiryagin M, Wolfs P, Cole C et al (2016) Design and Simulation of Heavy Haul Locomotives and Trains. CRC Press. https://doi.org/10.1201/9781315369792-4
Wang ZL, Yang JP, Shi K, et al (2022) Recent advances in researches on vehicle scanning method for bridges. Int J Struct Stab Dyn 22(15). https://doi.org/10.1142/s0219455422300051
Xin T, Wang P, Ding Y (2019) Effect of long-wavelength track irregularities on vehicle dynamic responses. Shock Vib 2019:1–11. https://doi.org/10.1155/2019/4178065
Xin Y, Hao H, Li J (2019) Time-varying system identification by enhanced empirical wavelet transform based on synchro-extracting transform. Eng Struct 196. https://doi.org/10.1016/j.engstruct.2019.109313
Yang YB, Yau JD (2017) Resonance of high-speed trains moving over a series of simple or continuous beams with non-ballasted tracks. Eng Struct 143:295–305. https://doi.org/10.1016/j.engstruct.2017.04.022
Yang YB, Lin CW, Yau JD (2004) Extracting bridge frequencies from the dynamic response of a passing vehicle. J Sound and Vib 272(3–5):471–493. https://doi.org/10.1016/s0022-460x(03)00378-x
Yang YB, Cheng MC, Chang KC (2013) Frequency variation in vehicle–bridge interaction systems. Int J Struct Stab Dyn 13(02). https://doi.org/10.1142/s0219455413500193
Youcef K, Sabiha T, El Mostafa D et al (2013) Dynamic analysis of train-bridge system and riding comfort of trains with rail irregularities. J Mech Sci Technol 27(4):951–962. https://doi.org/10.1007/s12206-013-0206-8
Yu G, Yu M, Xu C (2017) Synchroextracting transform. IEEE Trans Ind Electron 64(10):8042–8054. https://doi.org/10.1109/tie.2017.2696503
Zhai W, Sun X (2008) A detailed model for investigating vertical interaction between railway vehicle and track. Veh Syst Dyn 23(sup1):603–615. https://doi.org/10.1080/00423119308969544
Zhai W, Han Z, Chen Z et al (2019) Train-track-bridge dynamic interaction: a state-of-the-art review. Veh Syst Dyn 57(7):984–1027. https://doi.org/10.1080/00423114.2019.1605085
Zhai WM, Cai CB (2016) Train/track/bridge dynamic interactions: Simulation and applications. Veh Syst Dyn 37(sup1):653–665. https://doi.org/10.1080/00423114.2002.11666270
Zhang N, Tian Y, Xia H (2016) A train-bridge dynamic interaction analysis method and its experimental validation. Engineering 2(4):528–536. https://doi.org/10.1016/j.Eng.2016.04.012
Zhang TP, Zhu J, Xiong ZL, et al (2023) A new drive-by method for bridge damage inspection based on characteristic wavelet coefficient. Buildings 13(2). https://doi.org/10.3390/buildings13020397
Zhu Z, Gong W, Wang L et al (2017) A hybrid solution for studying vibrations of coupled train-track-bridge system. Adv Struct Eng 20(11):1699–1711. https://doi.org/10.1177/1369433217691775

Publisher's Note